CELL PRESERVATION TECHNOLOGY
Volume 2, Number 3, 2004

The Effect of Thermal Expansion of Ingredients on the Cocktails VS55 and DP6

JOSEPH PLITZ,[1] YOED RABIN,[1] and JOHN R. WALSH[2]

ABSTRACT

The formation of ice crystals is known to be lethal to biological cells. The presence of cryoprotectants at high cooling rates suppresses crystallization and promotes vitrification, where vitrification is solidification by rapid elevation of the viscosity (*vitreous*, in Latin, means glass). All materials have a tendency to change volume with a change in temperature, where the rate at which the volume changes with respect to the temperature is defined as the thermophysical property of thermal expansion. In the presence of a non-uniform temperature distribution in a bulky specimen, when different regions of the material tend to expand differently, mechanical stress may develop. It has been demonstrated that this mechanical stress can easily lead to macro structural damage to the cryopreserved specimen. As part of an ongoing effort to characterize the mechanical behavior of biological tissues and solutions in the cryogenic temperature range, the current study focuses on mapping the thermal expansion effect of cryoprotectants on the overall thermal expansion of cryoprotectant cocktails. Using a recently developed apparatus, the thermal expansion of the cryoprotectant components of the cocktails DP6 and VS55 were measured: propylene glycol, formamide, and DMSO. This paper includes a comparison of thermal expansion results with DSC analysis.

INTRODUCTION

CLASSICAL CRYOPRESERVATION, using relatively low concentrations of cryoprotective agents (cryoprotectants), has been shown to conserve many important properties of biological tissues—vascular allografts being a good example. However, the techniques developed for freezing vascular allografts are not reliable.[1,2] Fractures have been observed in cryopreserved arteries,[3] and similar observations have been made in recent studies of human arteries. In cryopreserved human internal mammary arteries and femoral arteries, both smooth muscle functions and endothelial functions were poorly preserved.[4,5]

Freeze-substitution of cryopreserved blood vessels demonstrates high levels of extra-cellular ice formation.[6] Classical cryopreservation, with low concentrations of DMSO, does a reasonable job of cell preservation by preventing intra-cellular ice formation, but it is a very poor method for preserving tissue. Even when all major cryopreservation variables are controlled, there is a limit—largely a function of tissue volume and geometry (including any immersion fluids and packaging)—beyond which traditional cryopreservation methods do not work consistently. There have been several hypotheses on the mechanisms of freezing-induced injury based upon a variety of factors,[7,8] but it has been discovered that the disadvantages of traditional cryopreservation revolve primarily around ice formation.[9–12]

Vitrification is an alternative to conventional freezing of living biological materials. Here, ice

[1]Department of Mechanical Engineering, Carnegie Mellon University, Pittsburgh, Pennsylvania.
[2]Organ Recovery Systems, Inc, Charleston, South Carolina.

formation is prevented because of the presence of high cryoprotectant concentrations that interact strongly with water. Vitrification does not have the biologically damaging effects associated with ice formation. No appreciable degradation occurs over time in living matter trapped within a vitreous matrix, and vitrification is potentially applicable to all biological systems.[13–16] Vitrification is a relatively well-understood physical process, but its application to the preservation of biological systems is not without problems, as the high cryoprotectant concentration necessary to facilitate vitrification is potentially toxic. To limit the effects of toxicity, it is necessary to use the least toxic cryoprotectant and the minimum concentration that will permit glass formation (at cooling rates that are practical for bulky mammalian tissues).[14,15] Vitrification avoids the hazards of direct injury from the mechanical effects of ice formation and, indirectly, from the solution effect injury. However, new potential mechanisms of injury associated with the amorphous state have been identified and must be studied as an essential component of developing methods of cryopreservation for multicellular tissues. The hypothesis of this study is that the mechanical stress associated with thermal expansion and contraction is a major potential source for injury in large, vitrified biological specimens. Such mechanisms have not previously been considered in any detail nor have they been amenable to specific study.

Mechanical stress in a material is related to pressure; it is the force per unit area that pulls the material apart (tensile stress), or presses it together (compressive stress). The magnitude of stress is related to the deformation of that material. Engineers define deformation, or strain, as the change in geometric size relative to the initial size. Changes in size are often much smaller than the size itself, as is the case in cryopreservation. When a material is at its original length, with no force acting upon it, the stress is zero. However, stress increases as the material is strained, while being maintained at a constant temperature. The rate at which stress increases with increasing strain depends on the stiffness of the material (elastic modulus).

Changes of temperature produce another independent effect. Any material which is unrestrained will undergo a change in size (thermal strain) when subjected to a change in temperature. Materials in general—and tissues as they are cryopreserved in particular—shrink when they are brought from physiological temperature down to cryogenic temperatures (typically in the order of 0.01% per Celsius degree). The dependency of this thermal strain on temperature is largely unexplored. The aim of this study was to measure the thermal strain when no external forces are acting on the material.

As tissues are cryopreserved, they are externally free to strain. However, in practice, it is impossible to cool a tissue of realistic size uniformly; the outside surface decreases in temperature more rapidly than the inside. Each layer of tissue tends to shrink according to its local temperature, which would require that the outside tissue overlap the inner tissue. This cannot be tolerated; therefore, stresses and additional strains beyond the thermal strains arise to make the shrinkages compatible. The outside of the tissue is forced to shrink less and the inside to shrink more. The level of stresses that must arise to accommodate the differential shrinkage depends upon the stiffness and relaxation of the material. If these stresses are too severe, they can, potentially, produce fractures, as has been observed in the cryopreservation of bulky specimens. There are methods for predicting the stresses that arise because of nonuniform changes in temperature. These methods combine mathematical analysis with data that captures:

(1) the thermal strain resulting from uniform temperature changes, and
(2) the time-dependent response of stress-to-strain as a function of temperature.

Prior studies of stress development did not address realistic or optimized cryopreservation conditions in which cryoprotective agents promote vitrification. The development of such methods for cryopreservation applications is the subject matter of a parallel effort by the authors.[17–20] Stress development during vitrification is completely unexplored, although some phenomenological reports are available.[21]

As part of an ongoing effort to characterize the mechanical behavior of biological tissues and solutions in cryogenic temperatures, this study focused on thermal expansion measurements of cryoprotectants. Using a recently developed apparatus,[22] the thermal strain has been measured. The ratio of the change in volume, as a result of a temperature change to the initial volume, is defined as the "volumetric thermal strain." The "linear thermal strain" is a relative property, which is defined as one-third of the volumetric thermal strain (for simplicity, linear thermal strain and thermal strain will be synonymous in this text). The term "linear thermal expansion coefficient" is an absolute thermophysical property, which is defined as the rate of change of the linear thermal strain with temperature (for simplicity, "linear thermal expansion coefficient" and "thermal expansion" will be synonymous in this text). Our study was focused on mapping the thermal expansion effects of the components of the cocktails DP6 and VS55, which are of great interest in cryopreservation applications.[23]

MATERIALS AND METHODS

The apparatus for thermal expansion measurements used in this study was presented previously by Rabin and Bell,[22] as shown in Figure 1. In broad terms, the experimental apparatus comprises an enclosure containing a cryoprotectant at a cryogenic temperature, and air at room temperature. The part of this enclosure which is brought to cryogenic temperatures is called the "cooling chamber." The part of the enclosure which is kept at room temperature is the "pressure tube." The pressure tube and the cooling chamber are connected through a flexible tube filled with the same cryoprotectant. The volume of the flexible tube is negligible, compared to the volume of the cooling chamber.

This experimental apparatus can only be used at the upper part of the cryogenic temperature range, where the cryoprotectant behaves like a relatively low viscous fluid. Each cryoprotectant has a unique threshold, below which the current apparatus will not provide

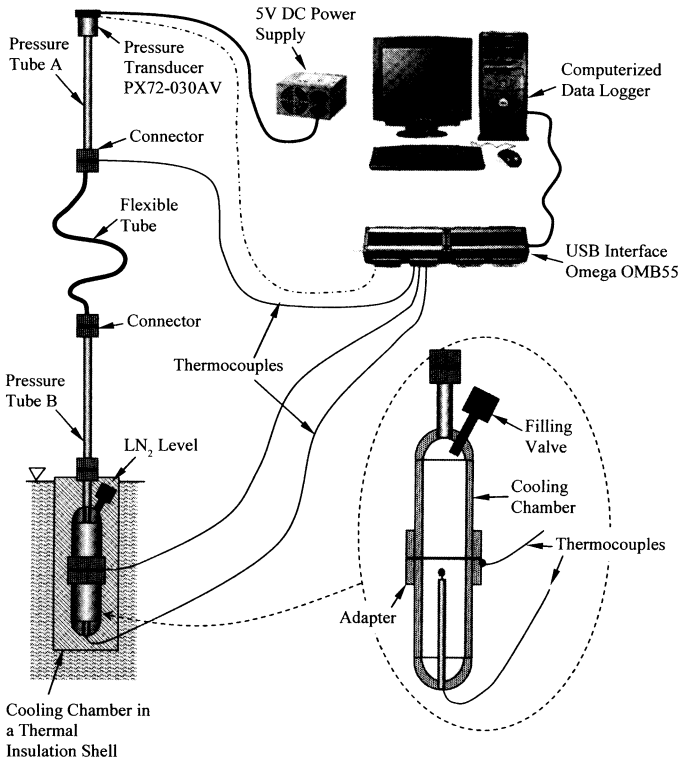

FIG. 1. Schematic illustration of the experimental apparatus. Reprinted from Rabin Y, Bell E. Thermal expansion measurements of cryoprotective agents. Part I; A new experimental apparatus. Cryobiology 2003;46:254–263. Copyright 2003, with permission from Elsevier.[22]

accurate measurements. This threshold is either at the onset of crystallization or at the point when the viscosity value becomes too high. The threshold for each cryoprotectant is addressed in the discussion section of this paper.

The measured parameters are the temperature of the cooling chamber and the air pressure change in the pressure tube. The calculated parameter is the thermal expansion that results in the respective pressure change. The thermal strain is conventionally defined in this study as:

$$\varepsilon = \frac{1}{3}\frac{\Delta V}{V} \quad (1)$$

where ΔV is the change in volume and V is the initial volume. The thermal expansion is defined as the derivative of the thermal strain with respect to temperature:

$$\beta = \frac{\partial \varepsilon}{\partial T} \quad (2)$$

Our study includes thermal expansion measurements of the ingredients of DP6 and VS55. DP6 is a cocktail of 234.4 g/L DMSO (3 M), 228.3 g/L propylene glycol (3 M), and 2.4 g/L HEPES in EuroCollins solution.[23] VS55 is a cocktail of 242.14 g/L DMSO (3.1 M), 168.38 g/L propylene glycol (2.2 M), 139.56 g/L formamide (3.1 M), and 2.4 g/L HEPES in EuroCollins solution. The two cocktails are similar, excepting the exclusion of formamide from DP6. In return, the DP6 contains a higher concentration of propylene glycol.

First, the cocktails DP6 (n = 4) and VS55 (n = 6) have also been tested. Next, four single-component cryoprotectant solutions, which are the ingredients of DP6 and VS55, have been tested: 3.1 M of DMSO (n = 5), 2.2 M of propylene glycol (n = 7), 3 M of propylene glycol (n = 8), and 3.1 M of formamide (n = 9). In order to save resources, 3.0 M of DMSO has not been tested; it was assumed that the thermal expansion of 3.0 M of DMSO could be approximated as the thermal expansion of 3.1 M of DMSO with 3% confidence (0.1 M difference divided by an absolute value of 3 M). In addition, three single-component solutions containing DMSO at higher concentrations have been tested: 6.0 M (n = 10), 7.05 M (n = 5), and 8.4 M (n = 9). The rationale for testing the higher concentration DMSO solutions is addressed in the discussion section of this paper.

Each single-component solution was prepared in 100-mL quantities. In preparing the solution, the solvent was added first. Next, 20 mL (or 20% of the total volume) of EuroCollins was added. Finally, water was added until the desired volume of 100 mL was achieved. Tap water was used in the thermal expansion measurements. Tap water is not typically used in cryobiology experiments for various reasons; however, because this study did not involve biological specimens, tap water was considered adequate.

Thermal properties of the cryoprotectant solutions were analyzed using differential scanning calorimetery (DSC). Sample aliquots of 5 μL were loaded into hermetically sealed aluminum sample pans, placed in a TA Instruments Q1000 MDSC, cooled to a minimum temperature well below the sample freezing point, or below the sample glass-transition temperature, and rewarmed to 10°C. All samples were thermally processed, according to average cooling and warming rates recorded during thermal expansion experiments for each solution.

RESULTS AND DISCUSSION

A typical thermal history of 3.1 M of DMSO during a thermal expansion experiment is shown in Fig. 2. Two temperature sensors are placed in the cooling chamber—one at the center of the cooling chamber, measuring the core cryoprotectant temperature, and one sensor measuring the temperature of the cooling chamber wall. With reference to Figure 2, the temperature of the cryoprotectant does not monotonically decrease with time in the cooling phase of the experiment. Point A in Figure 2 refers to a supercooling process, in which the material exists in the liquid phase below its equilibrium freezing point. Supercooling is an unstable condition, and is dependent on the cooling rate and the viscosity of the material. Point B refers to the crystallization of the material, which brings the tested solution to a stable state in the thermodynamic sense. The en-

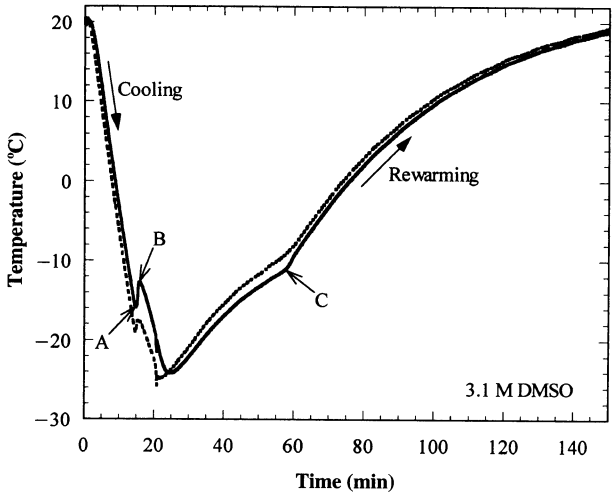

FIG. 2. Typical thermal history during a thermal strain experiment on 3.1 M of DMSO. The dashed line represents the temperature at the cooling chamber wall, while the solid line represents the specimen temperature at the center of the chamber. Points A and B refer to a supercooling process, in which the material exists in the liquid phase below its equilibrium freezing point (**A**), and subsequently crystallizes (**B**). Point C refers to melting.

ergy required for crystallization warms the solution between points A and B.

It is noted that 3.1 M of DMSO freezes over a temperature range, and not at a unique temperature value (note that the so-called "eutectic point" for DMSO is around 9.8 M of DMSO). It is further noted that point B in Figure 2, which is the upper boundary for freezing in this experiment, is lower than the upper boundary of melting of the same solution, as can be seen from Figure 3. Figure 3 shows a typical pressure-versus-temperature curve for 3.1 M DMSO of the same experiment shown in Figure 1. Point C in Figure 3 refers to an approximated upper boundary for melting the solution. The underlying assumption here is that the thermal expansion of the solution in the liquid state does not depend on whether the solution is cooled or rewarmed. Hence, point C is defined as the temperature at which the thermal expansion during rewarming returns to its value during cooling.

Figure 6 shows the best-fit polynomial approximation for the thermal strain, for DP6 and VS55, and all their ingredients. The coefficients of the polynomial approximations are listed in Table 1. The upper melting point (point C on Fig. 3) for the various solutions is also listed in Table 1, based on these thermal expansion measurements. It can be seen that the linear thermal strains of the various solutions are similar for a similar concentration around 3.1 M. The density of formamide, propylene glycol, and DMSO are 1.132, 1.036, and 1.100 g/mL, respectively, at 20°C.[24] It follows that the density of 3.1-M solutions of formamide, propylene glycol, and DMSO are 1.015, 1.006, and 1.021 g/mL, respectively, at 20°C (note that the density difference between these solutions is of the order of up to 1%). The molecular weight of formamide, propylene glycol, and DMSO are 45.04, 76.1, and 78.13, respectively.[24] The observation that the thermal expansion is dependent on either the molar concentration or the density of the solution—but not on the molecular weight—is intriguing.

It can be seen from Figure 6 that the linear strain of 8.4 M of DMSO is about 3% when cooled from an initial temperature of 20°C down to a temperature of −100°C. This results in a volumetric strain (contraction) of 9% over the respective temperature range. Since it is well established that mammalian cells can tolerate up to a 30% shrinkage during cryoprotectant addition and subsequent dehydration, it could be argued that the volume contraction of the cryoprotectant is insignificant with respect to the volume change the cell can tolerate. However, the rationale in this study was

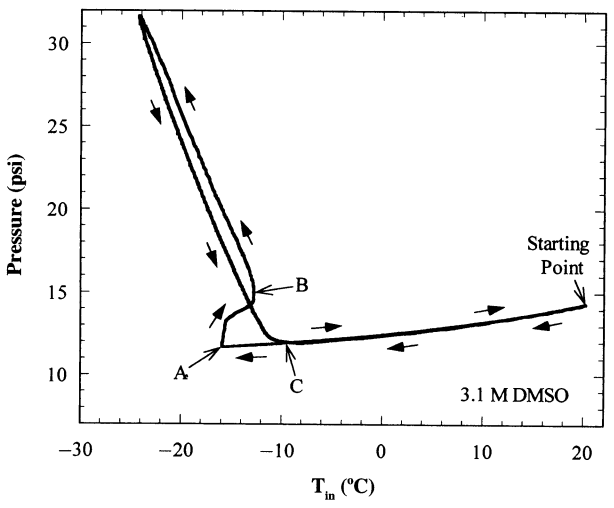

FIG. 3. Typical pressure measurements during a thermal strain experiment on 3.1 M of DMSO. Results shown in this figure correspond to the thermal history shown in Figure 2.

TABLE 1. COEFFICIENTS FOR BEST-FIT SECOND-ORDER POLYNOMIAL APPROXIMATION OF THERMAL STRAIN

Cryoprotectants concentration	a_2	a_1	a_0	σ	T_C, °C
2.2 M Propylene glycol	1.6767×10^{-6}	5.8305×10^{-5}	-1.9229×10^{-3}	6.086×10^{-5}	−4.1
3 M Propylene glycol	1.4532×10^{-6}	8.4701×10^{-5}	-2.3457×10^{-3}	4.777×10^{-5}	−6.6
3.1 M Formamide	1.3333×10^{-6}	8.4944×10^{-5}	-2.0004×10^{-3}	4.965×10^{-5}	−3.4
3.1 M DMSO	9.3242×10^{-7}	9.5570×10^{-5}	-1.9827×10^{-3}	1.127×10^{-4}	−7.7
6.0 M DMSO	2.2961×10^{-7}	1.9809×10^{-4}	-4.6086×10^{-3}	2.005×10^{-4}	−36.2
7.05 M DMSO	-9.7785×10^{-8}	2.0205×10^{-4}	-5.3834×10^{-3}	4.274×10^{-4}	−89.1
8.4 M DMSO	-1.0140×10^{-7}	2.3831×10^{-4}	-5.2052×10^{-3}	4.299×10^{-4}	−95.6
DP6	4.0963×10^{-7}	1.9224×10^{-4}	-3.4894×10^{-3}	6.917×10^{-5}	−29.8
VS55	9.4751×10^{-8}	1.9563×10^{-4}	-4.3474×10^{-3}	7.464×10^{-4}	−40.3

The linear thermal strain is approximated as $\varepsilon = a_2T^2 + a_1T + a_0$; σ is the standard deviation, and T_C is the temperture above which the cryoprotectant behaves like a liquid.

Following Eq. (2), the thermal expansion coefficient is: $\beta = 2a_2T + a_1$.

to model the thermal contraction of the cryoprotectant solution for the purpose of mechanical analysis, and not for the purpose of cell contraction tolerance in a fluid environment.

In order to illustrate the potential for structural damage driven by the cryoprotectant thermal expansion, assume the following thought experiment, where a sample of 8.4 M of DMSO is completely vitrified in a 50 mL vial, and stored at −120°C (a few degrees above the glass-transition temperature). Further assume that a miniature electrical heater was placed at the center of the vial prior to cooling, so as to heat the sample at a high enough rate, so as to prevent devitrification or recrystallization during the rewarming stage of the cryopreservation protocol. Finally, assume that the electrical heater reaches the temperature of 20°C when the vial-wall temperature is still well below −100°C, a temperature below which the cryoprotectant can be considered to be solid from mechanical considerations. The volume strain at the center of the sample in this experiment will exceed 9% (as evident from Fig. 6), which will cause an enormous elevation of hydrostatic pressure at the center of the vial. In turn, this will result in enormous stresses on the outer layer of the sample, which is still considered to be solid from a mechanics consideration. Most solid materials—and especially brittle materials such as the vitrified cryoprotectant—are not likely to sustain stress associated with a 9% volume change, and the potential to fracture increases dramatically, possibly leaving structural damage in the sample. The use of an electrical heater in the above thought experiment is for simplicity in presentation only; similar effects are likely be created without the use of an electrical heater, but in more complex geometries. Although this is a qualitative experiment only, fractures are indeed observed in large-scale vitrification, and the above thought experiment provides a plausible explanation for at least some of them.

Interestingly, ice crystallization is associated with a 9% volume change, and, as a result, it is very frequently associated with fracture formation. While ice crystallization and glass formation are inherently different phenomena, the solid material in either process will fail at similar in magnitude volumetric strains.

Another interesting phenomenon observed in the current study is associated with the naturally dissolved gasses in tap water. Frequently, the thermal strain in the liquid state during rewarming appeared similar to the thermal strain during cooling, but with a constant shift. The dissolved gases, mostly O_2, do not change the volume of a water sample, and do not affect its thermal expansion in the liquid state. During freezing, however, water molecules rearrange in a rigid structure to form crystals, while pushing away the dissolved gas molecules. These gas molecules form bubbles, which can be easily observed in ice cubes with a naked eye. During rewarming, most of the dissolved gases that escaped the liquid during solidification did not return into the liquid, but rather stayed in the form of microbubbles. Al-

though the overall volume of these bubbles is insignificant compared to the volume of the cooling chamber, the measured parameter here is the change in volume, and not the volume itself. The device used in this study was extremely sensitive and could measure the volume change resulting from microbubble formation, which is measured in quantities smaller than microliters for the chamber volume of 11 mL.

The constant shift in thermal strain was found in the first cooling/rewarming cycle on a given sample. If the experimentation on the same sample was repeated, this shift in thermal strain disappeared. Either way, since the thermophysical property of thermal expansion is the gradient of the thermal strain, and not the thermal strain itself, a strain offset between cooling and rewarming bears no effect on thermal-expansion calculations. Note that all thermal-expansion calculations in this paper are based on the cooling phase of each experiment.

High concentration DMSO versus VS55 and DP6

From Figure 6, it can be seen that the thermal strain of the different cryoprotectants is similar for a concentration of about 3 M. At higher concentrations, we hypothesized that the thermal strain is primarily a function of either the molar concentration or the total mass of solutes—and not of the particular cryoprotectant type—for the various cryoprotectants under investigation. To verify this hypothesis, three additional sets of experiments have been added: 6.0 M of DMSO, 7.05 M of DMSO, and 8.4 M of DMSO. The rationale is that 6.0 M and 8.4 M are the overall molar concentrations of all ingredients in DP6 and VS55, respectively. Furthermore, the 6.0 M- and 7.05-M DMSO solutions contain the same overall mass of solutes as in the cocktails DP6 and VS55, respectively.

Figures 3, 4, and 5, show the typical pressure measurements for DMSO concentrations of 3.1 M, 6.0 M, and 8.4 M, respectively. From the 3.1-M DMSO experiment, strong evidence of crystallization can be seen, which is associated with a dramatic thermal expansion upon freezing (Fig. 3). No dramatic event takes place during the cooling of the 6.0-M DMSO experiment (Fig. 4). However, expansion followed by contraction is evident at the beginning of the rewarming phase of 6.0 M of DMSO. The latter observation is likely to be associated with crystal formation during rewarming (devitrification), and/or with crystal growth around nuclei already present in the solid-like material (recrystallization). No dramatic event was observed in the 8.4-M DMSO experiment, which is likely to be associated with true vitrification (Fig. 5). Experiments with 7.05 M of DMSO produced similar results to those presented for 8.4 M of DMSO.

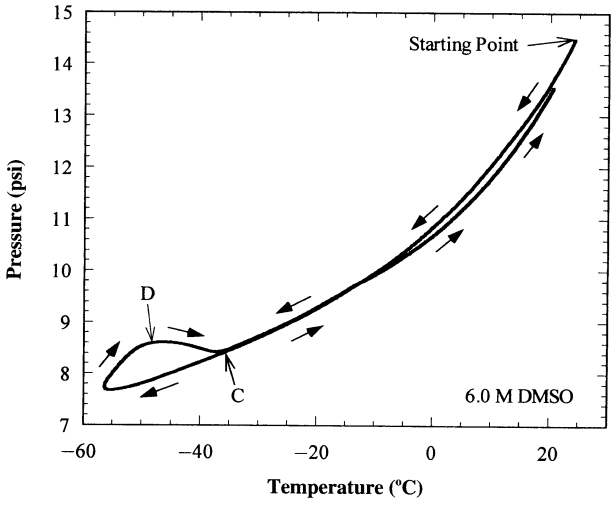

FIG. 4. Typical pressure measurements during a thermal strain experiment on 6.0 M of DMSO.

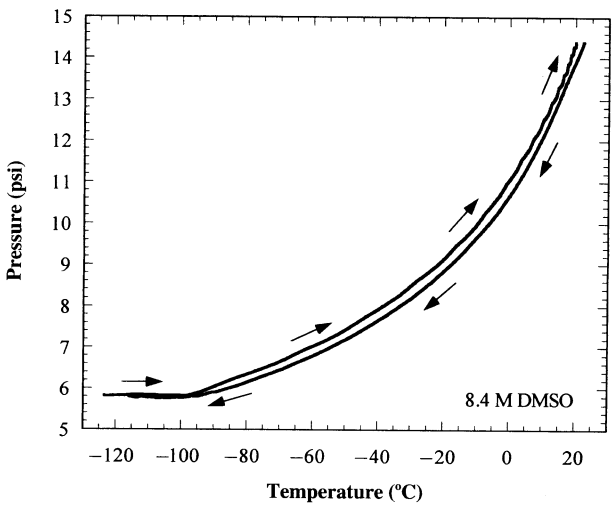

FIG. 5. Typical pressure measurements during a thermal strain experiment on 8.4 M of DMSO.

Figure 6 shows the average linear thermal strain of all experiments done for each concentration of DMSO. Figure 6 also shows the linear thermal strain of DP6 and VS55, which deviate by approximately 5% from previously reported measurements.[23] This difference is within the estimated range of uncertainty of the experimental apparatus, where $\delta\varepsilon = 3.3 \times 10^{-4}$.[23] It can be seen that the increase in DMSO concentration leads to an increase in the slope of the thermal strain—i.e., an increase in the thermal expansion in the range of concentrations studied here. It can bee seen from Figure 6 that the thermal strain results of 6.0 M of DMSO, 7.05 M of DMSO, DP6, and VS55 are found in a relatively narrow range, which is within the uncertainty range of VS55 measurements, for example ($\pm 2\delta\varepsilon$). However, the thermal strain results of 8.4 M of DMSO deviate significantly from measurements of the other solutions. This observation rejects the hypothesis that thermal expansion of the cryoprotectants under investigation is primarily a function of the molar concentration. This observation indicates that the thermal expansion is not a strong function of the total mass of solutes, in a mass range of 500 ± 50 g/L.

The outstanding observation here is that DP6, VS55, 6 M of DMSO, and 7.05M DMSO have similar behavior in terms of thermal strain, within the typical certainty of measurements that can be obtained using the specific experimental system. Furthermore, 7.05 M of DMSO shows a very close thermal expansion behavior to VS55, but is much easier to vitrify at the low cooling rates applied in this study (see the DSC studies section below). These observations will have a great impact on future studies of solid mechanics. For example, if either 6.0 M of DMSO, 7.05 M of DMSO, or any other concentration of DMSO solution within this range is found to have a similar viscosity value to VS55, these could be considered equivalent from solid-mechanics considerations, and would, thereby, simplify future analyses.

Finally, Figure 7 presents the approximated thermophysical property of thermal expansion for each solution, which is the derivative of the thermal strain, Eq. (2). Note that the thermal expansion is measured indirectly, which may affect its level of certainty. On the other hand, the thermal strain—and not the thermal expansion—is taken into account in solid-mechanics analyses.

DSC verification of DMSO experiments

Point C in Figures 3 and 4 indicates the temperature above which the material returns to

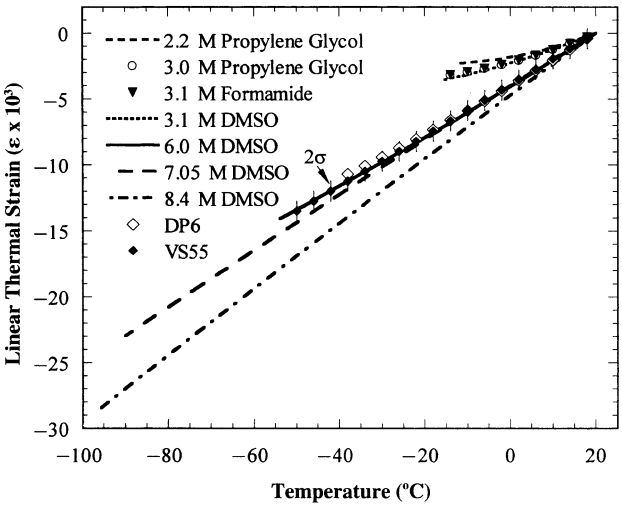

FIG. 6. Best-fit polynomial approximation of the linear thermal strain of the ingredients of DP6 and VS55, the cocktails DP6 and VS55, and higher concentrations of DMSO. The best-fit approximation is based on the cooling phase in each experiment. The error bars on the VS55 represent $\pm 2\delta\varepsilon$.[23] Coefficients and standard deviation values for all curves are listed in Table 1.

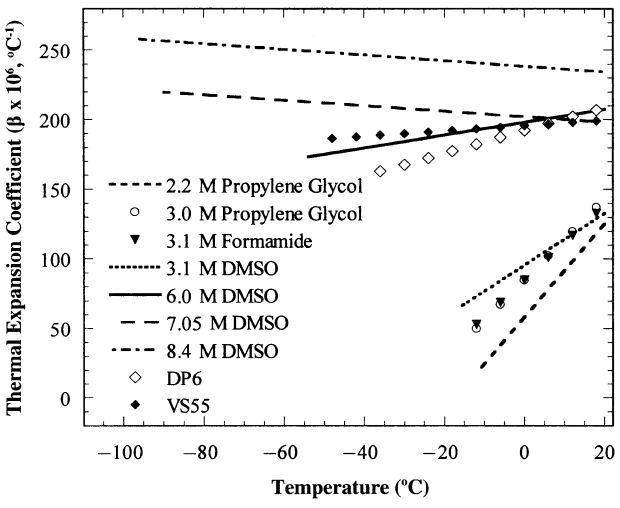

FIG. 7. Best-fit polynomial approximation of the thermal expansion of the ingredients of DP6 and VS55, the cocktails DP6 and VS55, and higher concentrations of DMSO. The best-fit approximation is based on the cooling phase in each experiment. The coefficients are listed in Table 1.

behave like liquid in the fluid-mechanics sense. In order to verify this interpretation of experimental results, an additional series of DSC experiments was conducted. These experiments included 3.1 M, 6.0 M, 7.05 M, and 8.4 M of DMSO, in typical cooling and rewarming rates measured during the thermal-expansion experiments.

The thermal behavior of the cooling chamber can be approximated as a lumped system, characterized by a close-to-uniform temperature, represented by a single temperature value at any given point in time. It can be seen from Figure 2 that a lumped-system approach is a good approximation for the cooling chamber, where the two temperature curves represent the boundaries for the temperature distribution in the system. The supercooling effect makes the lumped-system assumption somewhat weaker, but only around the freezing temperature. In a convective environment, a lumped system would display an exponential decay in temperature, from an initial temperature value to the surroundings temperature.

The first scheme for the DSC experiments was to follow exactly the thermal history of the cooling chamber, as recorded during the thermal expansion studies (Fig. 3, for example). The DSC device used in this study can be programmed with a series of up to 7 ramps, which is deemed adequate for this task. Unfortunately, changing cooling rates (i.e., ramp values) during the DSC experiment created artifacts, which overwhelmed the expected readings. These artifacts were associated with the settlement time of the control system after changing a ramp value. Taking into account that the desired ramp value changes were planned at the critical thermal points under investigation, such as points A, B, or C, in Figure 3, this attempt failed to produce the desired outcome.

Consequently, a second scheme was developed for the DSC studies. The aim in this scheme was to measure the melting point, or the melting range, during rewarming. The melting point is considered to be one of the most important parameters in fluid-mechanics analyses, above which the material behaves like liquid, both during cooling and rewarming. Note that the solidification temperature and the effect of supercooling are, to a large extent, functions of the specimen size, while melting is expected to be unaffected by the size of the specimen. In this attempt, the suspected temperature for melting completion, T_C, was first identified from the pressure-versus-temperature curves of the thermal-expansion measurements (Fig. 3, for example). Next, the rewarming rate, H_2, was calculated when the specimen temperature approached T_C, using the thermal history curve (Fig. 2, for example). The average initial cooling rate, H_1, between the T_C value during cooling and the minimum temperature achieved, T_{min}, was also calculated from the same thermal-history curve. Finally, the DSC thermal protocol included: equilibration of the specimen at 10°C (well above freezing/melting), cooling at a rate of H_1 down to T_{min}, equilibration for two min at T_{min}, and rewarming at a rate of H_2 back to 10°C.

Results of the DSC experiments from the second scheme are listed in Table 2. Here, T_m is the upper boundary of melting, based on the DSC analysis, while T_C represents the same boundary, based on thermal-expansion measurements. An average difference of 0.6°C was found between T_m and T_C for 3.1 M of DMSO. Given the size of the sample and the two inherently different measurement techniques, a very good agreement of results can be observed.

For 6.0 M of DMSO, no crystallization can be identified, based on both DSC analyses and thermal-expansion measurements. Devitrification or recrystallization and subsequent melting were observed in some DSC studies of 6.0 M of DMSO, and can also be seen in Figure 4, from thermal-expansion experiments. Neither was the effect of recrystallization nor of devitrification highly repeatable in thermal-expansion experiments, possibly because the particular concentration of 6.0 M is a boundary value, which merely leads to devitrification or recrystallization at the particular rewarming rate used in the thermal-expansion measurements. Note that devitrification and recrystallization are statistical events, which are less likely to happen in a DSC chamber size of 20 μL than in the bulky cooling chamber size of 11.1 mL. For cases where the melting of 6.0 M of DMSO was observed, an average difference of 0.8°C

TABLE 2. SUMMARY OF DSC RESULTS

DMSO solution	T_{min}	T_n	T_g	T_d	T_p	T_m	T_C	*Cooling rates*
3.1 M	−40.0	−38.1	n/o	n/o	−12.3	−8.1		
	−40.0	−36.1	n/o	n/o	−12.6	−8.2	−7.7	H_1 = −2.65°C/min
	−40.0	−37.6	n/o	n/o	−12.2	−8.5	(n = 5)	H_2 = +0.46°C/min
	−40.0	−36.6	n/o	n/o	−13.1	−8.3		
6.0 M	−80.0	n/o	n/o	n/o	n/o	n/o		
	−80.0	n/o	n/o	n/o	n/o	n/o		
	−80.0	n/o	n/o	−44.3	−35.5	−33.5	−36.2	H_1 = −1.58°C/min
	−120.0	n/o	n/o	−79.8	−39.6	−36.6	(n = 10)	H_2 = +1.40°C/min
	−150.0	n/o	−133.4	−81.5	−40.6	−37.0		
	−150.0	n/o	−133.4	−83.4	−40.0	−36.1		
	−150.0	n/o	−132.3	n/o	n/o	n/o		
7.05 M	−150.0	n/o	−132.1	n/o	n/o	n/o	−89.1	H_1 = −1.40°C/min
	−150.0	n/o	−131.9	n/o	n/o	n/o	(n = 5)	H_2 = +2.28°C/min
	−150.0	n/o	−131.8	n/o	n/o	n/o		
	−150.0	n/o	−127.5	n/o	n/o	n/o		
8.4 M	−150.0	n/o	−127.1	n/o	n/o	n/o	−95.6	H_1 = −1.40°C/min
	−150.0	n/o	−127.3	n/o	n/o	n/o	(n = 9)	H_2 = +2.28°C/min
	−150.0	n/o	−128.6	n/o	n/o	n/o		

Thermal protocol: starting from equilibration at 10°C, the specimen was cooled at a rate of H_1, down to T_{min}, held for 2 min at T_{min}, and rewarmed at a rate of H_2 back to the initial temperature.
n/o: The event was not observed.
T_n: Nucleation temperture observed during cooling, °C.
T_g: Glass transition temperature during rewarming, °C.
T_d: Devitrification/recrystallization temperature during rewarming, °C.
T_p: Peak melting temperature during rewarming, °C.
T_m: Melting-complete temperature during rewarming, °C.
T_C: The temperature above which the cryoprotectant behaves like a liquid, based on thermal expansion experiments, °C.

was found between DSC analysis and thermal-expansion measurements.

No crystallization or melting was observed with 7.05 M of DMSO and 8.4 M of DMSO, using either DSC measurements or thermal-expansion measurements. However, based on the thermal expansion measurements, the material could be considered liquid for practical purposes only above an average temperature of 89.1°C and 95.6°C for 7.05 M of DMSO and 8.4 M of DMSO, respectively, the reason being that the ability of vitrified material to flow decays exponentially with the decrease in temperature. In our investigation, no contraction was observed below 89.1°C and 95.6°C, respectively, although the material was expected to strain increasingly (contract) with the decrease in temperature.

SUMMARY AND CONCLUSIONS

This study focused on thermal-expansion measurements of the ingredients of the cocktails DP6 and VS55: 2.2 M of propylene glycol, 3.0 M of propylene glycol, 3.1 M of formamide, and 3.1 M of DMSO. This study also included thermal-expansion measurements of higher concentrations of DMSO solutions of 6.0 M, 7.05 M, and 8.4 M. Finally, our study also included a comparison of DSC analysis with thermal expansion results related to the upper boundary of melting of DMSO at various concentrations.

It was observed that the thermal expansion of 3.0 M of propylene glycol, 3.1 M of formamide, and 3.1 M of DMSO is relatively close. It was further observed that thermal expansion of DMSO increases with the increase in concentration—at least up to 8.4 M of DMSO. The most important observation is that the thermal expansion of 6.0 M of DMSO, 7.05 M of DMSO, VS55, and DP6 is in a relatively close range. This observation is not related to the molar concentration, nor to the molecular weight of the ingredient. It was further observed that the thermal expansion of DMSO at the respective concentration can be measured to a much lower

temperature than the thermal expansion of DP6 and VS55. These observations will have a great impact on future studies related to thermo-mechanical stresses.

A very good agreement was found in the identification of the upper boundary, of melting using a DSC device and the recently developed apparatus for thermal-expansion measurements. The comparison to DSC analyses was deemed necessary to verify our interpretation of thermal-expansion results. It was noted that the internal energy changes sensed by the DSC, and the thermal-expansion changes sensed by the device for thermal-expansion measurements, were directly related.

Results in this study are presented within the temperature range in which the material can be considered fluid for continuum mechanics analysis. The thermal-expansion phenomenon at temperatures approaching the glass-transition temperature is quite a complex phenomenon, and the simple fluid approach is not likely to be valid. In this temperature region, effects of structural relaxation are also involved in thermal expansion. Therefore, the extrapolation of the results presented in this study to lower temperatures requires careful attention.

ACKNOWLEDGMENTS

This study was supported, in part, by NHLBI, grant # R01 HL069944-01A1. This research was also supported, in part, by Organ Recovery Systems, Inc., Charleston, SC. The authors would like to thank Dr. Michael Taylor for the insightful discussions in the course of this study.

REFERENCES

1. Almassi GH, Farahbakhsh B, Wooldridge T, et al. Endothelium and vascular smooth muscle function in internal mammary artery after cryopreservation. J Surg Res 1996;60:355–360.
2. Nataf P, Hadjiisky P, Lechat P, et al. Effect of cold anoxia and cryopreservation on metabolic and contractile functions of human mammary artery. Cryobiology 1995;23:327–333.
3. Hunt CJ, Song YC, Bateson EAJ, et al. Fractures in cryopreserved arteries. Cryobiology 1994;31:506–515.
4. Muller-Schweinitzer E, Stulz P, Striffeler H, et al. Functional activity and transmembrane signaling mechanisms after cryopreservation of human internal mammary arteries. J Vasc Surg 1988;27:528–537.
5. Stanke F, Riebel D, Carmine S, et al. Functional assessment of human femoral arteries after cryopreservation. J Vasc Surg 1998;28:273–283.
6. Song YC, Khirabadi BS, Lightfoot FG, et al. Vitreous cryopreservation maintains the function of vascular grafts. Nat Biotechnol 2000;18:296–299.
7. Karow AM. Biophysical and chemical considerations in cryopreservation. In: Karow AM, Pegg DE, eds. *Organ Preservation for Transplantation*. New York: Dekker; 1981:113.
8. Mazur P. Freezing of living cells: Mechanisms and implications. Am J Physiol 1984;247:125.
9. Pegg DE, Jacobsen IA, Armitage WJ, et al. Mechanisms of cryoinjury in organs. In: Pegg DE, Jacobsen IA, eds. *Organ Preservation II*. Edinburgh, United Kingdom: Churchill Livingstone; 1979:132–146.
10. Pegg DE. Principles of tissue preservation. In: Morris PJ, Tilney NL, eds. *Progress in Transplantation*. Edinburgh, United Kingdom: Churchill Livingston; 1985: 69–105.
11. Pegg DE. Ice crystals in tissues and organs. In: Pegg DE, Karow AM, Jr., eds. *The Biophysics of Organ Preservation*. New York: Plenum Publishing Corp.; 1987: 117–140.
12. Taylor MJ. Sub-zero preservation and the prospect of long-term storage of multi-cellular tissues and organs. In: Calne RY, ed. *Transplantation Immunology: Clinical and Experimental*. Oxford New York Tokyo: Oxford University Press; 1984:360–390.
13. Fahy GM, MacFarlane DR, Angell CA, et al. Vitrification as an approach to cryopreservation. Cryobiology 1984;21:407–426.
14. Fahy GM, Levy D, Ali, SE. Some emerging principles underlying the physical properties, biological actions, and utility of vitrification solutions. Cryobiology 1987;24:196–213.
15. Fahy GM. Biological effects of vitrification and devitrification. In: Pegg DE, Karow AM, Jr., eds. *Biophysics of Organ Cryopreservation*. New York: Plenum; 1987: 265–297.
16. Fahy GM. Vitrification. In: McGrath JJ, Diller KR, eds. *Low Temperature Biotechnology:Emerging Applications and Engineering Contributions*. New York: ASME; 1988:113–146.
17. Pegg DE, Wustemanm MC, Boylan S. Fractures in cryopreserved elastic arteries: Mechanism and prevention. Cryobiology 1996;33:658–659.
18. Rabin Y, Steif PS. Analysis of thermal stresses around cryosurgical probe. Cryobiology 1996;33:276–290.
19. Rabin Y, Steif PS. Thermal stresses in a freezing sphere and its application to cryobiology. ASME J Appl Mech 1998;65:328–333.
20. Rabin Y, Steif PS. Thermal stress modeling in cryosurgery. Int J Sol Struct 2000;37:2363–2375.
21. Fahy GM, Saur J, Williams RJ. Physical problems with the vitrification of large biological systems. Cryobiology 1990;27:492–510.

22. Rabin Y, Bell E. Thermal expansion measurements of cryoprotective agents. Part I:A new experimental apparatus. Cryobiology 2003;46:254–263.
23. Rabin Y, Bell E. Thermal expansion measurements of cryoprotective agents. Part II:Measurements of DP6 and VS55, and comparison with DMSO. Cryobiology 2003;46:264–270.
24. Lide DR, ed. *CRC Handbook of Chemistry and Physics*, 75th ed. Boca Raton, FL: CRC Press; 1994.

Address reprint requests to:
Dr. Yoed Rabin
Department of Mechanical Engineering
5000 Forbes Avenue
Carnegie Mellon University
Pittsburgh, PA 15213

E-mail: rabin@cmu.edu